

Research Article: New Research | Disorders of the Nervous System

Numbers of granule cells and GABAergic boutons are correlated in shrunken sclerotic hippocampi of sea lions with temporal lobe epilepsy

<https://doi.org/10.1523/ENEURO.0389-25.2026>

Received: 21 October 2025

Revised: 25 February 2026

Accepted: 2 March 2026

Copyright © 2026 Wyeth et al.

This is an open-access article distributed under the terms of the [Creative Commons Attribution 4.0 International license](#), which permits unrestricted use, distribution and reproduction in any medium provided that the original work is properly attributed.

This Early Release article has been peer reviewed and accepted, but has not been through the composition and copyediting processes. The final version may differ slightly in style or formatting and will contain links to any extended data.

Alerts: Sign up at www.eneuro.org/alerts to receive customized email alerts when the fully formatted version of this article is published.

1
2
3
4
5
6
7
8
9
10
11
12
13
14
15
16
17
18
19
20
21
22
23
24
25
26
27
28
29
30
31
32
33
34
35
36
37
38
39
40
41
42
43
44
45
46
47
48
49

Numbers of granule cells and GABAergic boutons are correlated in shrunken sclerotic hippocampi of sea lions with temporal lobe epilepsy

Megan Wyeth, mwyeth@stanford.edu, Department of Comparative Medicine, Stanford University, Palo Alto, CA 94304

David D. R. Krucik, David.Krucik@outlook.com, Department of Comparative Medicine, Stanford University, Palo Alto, CA 94304.

Chloé J. Thorbrogger, chloethor@berkeley.edu, Department of Comparative Medicine, Stanford University, Palo Alto, CA 94304.

Cara Field, fieldc@TMMC.org, The Marine Mammal Center, 2000 Bunker Road, Sausalito, CA 94965

Paul S. Buckmaster, psb@stanford.edu, Departments of Comparative Medicine and Neurology & Neurological Sciences, Stanford University, Palo Alto, CA 94304

Corresponding author: Megan Wyeth, Stanford University School of Medicine, 3172 Porter Drive, Palo Alto, CA 94304, mwyeth@stanford.edu

288 Figures, 2 Tables

Abstract 207 words, Introduction 613 words, Discussion 1471 words

Acknowledgements

Supported by the National Science Foundation (OCE-131821), National Institute of Environmental Health Sciences (ES021960), National Institute of Neurological Disorders and Stroke (NS107290, NS136433), and National Institutes of Health Office of the Director (OD010989, OD011121). Animals were sampled under the Marine Mammal Protection Act permit number 18786.

Conflict of Interest Statement

The authors declare no competing financial interests.

The data that support the findings of this study are openly available in Dryad at <http://doi.org/DOI:10.5061/dryad.t4b8gtjd5>

50 Abstract

51 A possible mechanism of temporal lobe epilepsy is insufficient inhibition of hippocampal dentate
52 granule cells. Precipitating injuries that kill interneurons in the dentate gyrus might result in fewer
53 inhibitory synapses with granule cells. To test this hypothesis, previous studies evaluated numbers or
54 densities of interneurons, γ -amino butyric acid (GABA)ergic boutons, and inhibitory synapses in tissue
55 from human patients with temporal lobe epilepsy and rodent models. However, those studies have
56 limitations. Some of those limitations can be addressed by a large animal model. Sea lions (*Zalophus*
57 *californianus*) can develop temporal lobe epilepsy naturally. Like humans, epileptic sea lions exhibit
58 bilateral or unilateral hippocampal sclerosis (neuron loss) with granule cell vulnerability, but sea lions
59 permit optimal tissue preservation and sampling, and good control subjects. To label interneuron cell
60 bodies and GABAergic synaptic boutons, sea lion hippocampal tissue from both sexes was processed
61 with immunohistochemistry for glutamic acid decarboxylase (GAD) and vesicular GABA transporter.
62 Stereological techniques were used to evaluate the dentate gyrus of the entire hippocampus. Numbers
63 of granule cells, GAD cells, and GABAergic boutons were substantially reduced in shrunken, sclerotic
64 hippocampi. However, numbers of GABAergic boutons and granule cells were correlated. These
65 findings indicate that, despite losses, numbers of GABAergic boutons scale with numbers of surviving
66 granule cells.

67

68 Significance Statement

69 Temporal lobe epilepsy is a challenging clinical problem. Electrophysiological studies reveal that
70 hippocampal dentate granule cells are insufficiently inhibited and hyperexcitable in epileptic tissue from
71 humans and rodent models. The present stereological analysis of a large animal model (sea lions)
72 found no evidence for disproportionate loss of dentate gyrus GABAergic boutons in temporal lobe
73 epilepsy. These data suggest reduced inhibition of granule cells is attributable to something other than
74 too few GABAergic boutons.

75

76Introduction

77One of 26 people in the United States develops epilepsy at some time in their life (Hesdorffer et al.,
782011). Temporal lobe epilepsy is one of the most common types (Engel et al., 1997). The hippocampus
79is the most frequent site of seizure initiation (Quesney, 1986; Spencer et al., 1987, 1990; Sperling and
80O'Connor, 1989; Duckrow and Spencer, 1992; Spencer and Spencer, 1994; Masukawa et al., 1995;
81King et al., 1997; Wennberg et al., 2002). Normally, the hippocampal dentate gyrus has gate-like
82properties that resist seizure activity (Lothman et al., 1991; Heinemann et al., 1992; Krook-Magnuson et
83al., 2015). However, in patients with temporal lobe epilepsy the dentate gyrus displays neuropathology
84(Margerison and Corsellis, 1966), including loss of inhibitory interneurons (de Lanerolle et al., 1989;
85Sloviter et al., 1991; Mathern et al., 1995; Zhu et al., 1997; Maglóczy et al., 2000; Andrioli et al., 2007;
86Tóth et al., 2010).

87

88In hippocampal slices prepared from tissue resected to treat patients, the dentate gyrus can generate
89seizure activity (Gabriel et al., 2004; Jandová et al., 2006), and granule cells are hyperexcitable
90(Isokawa and Levesque, 1991; Isokawa et al., 1991) largely because of reduced inhibition (Masukawa
91et al., 1989; Franck et al., 1995; Isokawa, 1996; Williamson et al., 1999). Deficits of granule cell
92inhibition also have been reported in rodent models of temporal lobe epilepsy (Sayin et al., 2003;
93Pathak et al., 2007; Sun et al., 2014; Dengler et al., 2017). For example, γ -amino butyric acid
94(GABA)ergic synaptic input to granule cells, measured as miniature inhibitory postsynaptic current
95frequency, is markedly reduced (Kobayashi and Buckmaster, 2003; Shao and Dudek, 2005; Sun et al.,
962007).

97

98Interneuron loss may reduce the number of GABAergic synapses with granule cells, resulting in less
99inhibition, hyperexcitability, and seizures. The hypothesis is consistent with efficacy of anti-seizure
100drugs that augment GABAergic synaptic function (Greenfield, 2013), with evidence that promoting
101inhibitory synaptogenesis decreases epileptiform activity (Adel et al., 2023), and with reduced seizure
102frequency after transplanting GABAergic cells into the hippocampus in rodent models of temporal lobe

103epilepsy (Hunt et al., 2013; Casalia et al., 2017; Upadhyaya et al., 2019; Zhu et al., 2023). Contrary to the
104hypothesis, studies of tissue from patients with temporal lobe epilepsy (Babb et al., 1989; Wittner et al.,
1052001; Wittner and Maglóczy, 2017; Alhourani et al., 2020) and rodent models (Thind et al., 2010) have
106reported more, not fewer, GABAergic boutons or inhibitory synapses per granule cell. However, the
107evidence against the hypothesis has limitations. Some of those limitations can be addressed by a large
108animal model.

109

110California sea lions are a large animal model of temporal lobe epilepsy (Buckmaster, 2017). Adult sea
111lions (*Zalophus californianus*) weigh up to 220 (females) or 850 pounds (males). Their gyrencephalic
112brain is one-quarter the size of a human brain. During naturally occurring oceanic algal blooms sea
113lions are exposed by diet to the kainic acid receptor agonist domoic acid, which can result in status
114epilepticus. Some surviving sea lions develop temporal lobe epilepsy. Epileptic sea lions have a poor
115prognosis and are euthanized to avoid suffering. These sea lions reproduce the neuropathology of
116human patients, including unilateral hippocampal sclerosis in many cases and partial loss of granule
117cells (Buckmaster et al., 2014; Cameron et al., 2019), which is an advantage over rodent models. Sea
118lion tissue is not limited by constraints of human studies including small sample sizes, inadequate
119controls, limited tissue sampling, or compromised tissue preservation. The present study used
120immunohistochemistry and stereological techniques to evaluate GABAergic neurons and boutons in the
121dentate gyrus of entire hippocampi in sea lions with temporal lobe epilepsy to test the hypothesis that
122there is disproportionate loss of GABAergic boutons relative to granule cells.

123

124**Materials and Methods**

125This experiment used brain tissue of sea lions (*Zalophus californianus*) from a previous study that
126reports details on subjects and methods of perfusion and sectioning (Cameron et al., 2019). Subjects
127included those stranded along the California coast who were admitted to The Marine Mammal Center
128for rehabilitation but did not respond to treatment and were euthanized due to poor prognosis for
129release. Of 29 sea lions in the present study 19 were female (sex was undetermined in one). Ages

130included 1 pup, 2 yearlings, 4 juveniles, 6 subadults, and 16 adults. Hippocampal sclerosis was
131identified by severe hilar neuron loss (Buckmaster et al., 2014; Cameron et al., 2019). Spontaneous
132seizures were witnessed in 9 of 16 sea lions with hippocampal sclerosis. Control sea lions (n=13) did
133not have hippocampal sclerosis, and reasons for euthanasia included trauma and infection.
134Immediately upon euthanasia by pentobarbital overdose, sea lions were perfused through the
135ascending aorta (1 L/min) with 0.9% NaCl for 2 min, followed by 4% formaldehyde in phosphate buffer
136(PB) for 30 min. Brains were bisected and each hemisphere cut into ~2 cm thick coronal blocks for
137post-fixing in 4% formaldehyde with 30% sucrose in PB at 4°C. After equilibrating for a week, blocks
138were frozen in isopentane and stored at -80°C. Sections (40 µm) from a sliding microtome were stored
139in cryoprotective solution at -20°C until processing for immunohistochemistry.

140

141Both hippocampi of all subjects were evaluated with three stains: the Nissl stain thionin, glutamic acid
142decarboxylase (GAD)-immunoreactivity to visualize interneuron cell bodies, and GAD- and vesicular
143GABA transporter (VGAT)-immunoreactivity to identify GABAergic synaptic boutons (Figure 1).
144Sections processed for bouton staining were lightly counterstained with thionin to facilitate granule cell
145layer identification.

146

147Previously, a 1-in-40 series of coronal sections (starting at a random point near the temporal pole, on
148average 10.3 sections/hippocampus) was stained with thionin to stereologically estimate the number of
149granule cells per hippocampus and identify sclerotic hippocampi based on severe hilar neuron loss
150(Cameron et al., 2019; Table 1). Those data were used in the present study, which also processed
151another 1-in-40 series of sections for GAD67-immunoreactivity using a staining protocol optimized to
152label interneuron cell bodies. Free-floating sections were washed in 1% hydrogen peroxide in 0.05 M
153tris-buffered saline (TBS), rinsed, and pre-incubated in blocking solution containing 3% normal goat
154serum (NGS) and 2% bovine serum albumin (BSA) in TBS. Sections were transferred to a primary
155solution with anti-GAD67 (1:1000, Millipore No. MAB5406), 1% NGS and 0.2% BSA for 1 week at 4°C.
156Sections were rinsed and incubated for 2 h in a secondary solution composed of goat anti-mouse

157(1:500, Vector Laboratories No. BP-9200, RRID:AB_2827937) and 2% BSA in TBS, followed by 2 h in
158Vectastain Elite ABC-HRP (1:500 in TBS, Vector Laboratories) with 2% BSA. Finally, sections were
159processed for visualization with 2% diaminobenzidine tetrahydrochloride in 0.1 M Tris buffer, mounted,
160dehydrated, and coverslipped.

161

162Another 1-in-40 series of sections was processed with a staining protocol optimized to label GABAergic
163synaptic boutons. In the interest of labeling GABAergic boutons as completely as possible, pilot studies
164tested numerous antibodies in sea lion tissue. Antibodies that produced optimal labeling of boutons
165were to GAD65/67 (1:3000, L127/12, UC Davis/NIH NeuroMab Facility) and to VGAT (1:2000,
166MSFR106160, Frontier Institute). Previous studies revealed robust GABAergic bouton labeling when
167antibodies to GAD and VGAT were combined (Alhourani et al., 2020). In the present study, tissue was
168processed with both antibodies combined to avoid missing boutons that might be labeled only by one.
169The immunohistochemistry protocol was the same as for GAD67, apart from the addition of 0.3% triton
170to the blocking, primary, secondary, and ABC solutions, and the inclusion of goat anti-guinea pig serum
171(1:500, Vector Laboratories No. BA-7000, RRID:AB_2336132) in the secondary solution.

172

173Antibody Characterization

174The well-established monoclonal antibody to GAD67 used here (clone 1G10.2, RRID:AB_2278725)
175was raised in mouse against the 67 kDa human isoform (amino acids 4-101). It produces a single band
176by immunoblot and has no cross reactivity with the 65 kDa isoform from rat brain (Fong et al., 2005).
177Immunoreactivity was eliminated in the brain of a Gad1 knockout rat (Fujihara et al., 2020). Cell
178labeling was similar to adjacent sections of rat brainstem processed for in situ hybridization (Fong et al.,
1792005). Importantly, the labeling in sea lion produced the expected pattern of cell bodies in the dentate
180gyrus based on in situ hybridization in rat (Houser and Esclapez, 1994; Esclapez and Houser, 1999).

181

182Polyclonal anti-VGAT (RRID:AB_2571624) was raised in guinea pig against a fusion protein for mouse
183VGAT (amino acids 31-112). Immunoblot detected a single protein band at ~57 kDa (Fukudome et al.,

1842004) as expected (Chaudhry et al., 1998). The expression in interneuron boutons of sea lion
185hippocampus corresponded to the labeling pattern in rats (Chaudhry et al., 1998; Boulland et al., 2007).
186
187Monoclonal anti-GAD65/67 (clone L127/12, RRID:AB_2756510) was raised in mouse against the full
188length (amino acids 1-594) fusion protein of human GAD67. It has a molecular weight of ~70 kDa and
189cross-reacts with GAD65 (60% identity, highest in the C-terminus, manufacturer's datasheet). The
190staining pattern of interneuron boutons in sea lion hippocampus matched previous reports in rats
191(Ribak et al., 1978; Fukuda et al., 1998).

192

193Microscopic analysis

194To analyze the distribution of interneurons across layers and along the septotemporal axis of the
195dentate gyrus, all GAD-positive cell body profiles were marked using Stereo Investigator (MBF
196Bioscience). To estimate the number of dentate gyrus GAD cells, the optical fractionator method was
197used (Table 1). Contours were drawn around the entire dentate gyrus: hilus, granule cell layer, and
198molecular layer. Cells were visualized with a 63X Plan-Apochromat 1.4 na lens (Zeiss). Cell bodies that
199were not cut at the section surface and began coming into focus while focusing down through the
200section were counted. Counting grid size depended on hippocampus size. Shrunken, sclerotic
201hippocampi were evaluated with a smaller grid so that enough cells could be counted. The Cavalieri
202method was used with area measurements from contours drawn around the dentate gyrus to estimate
203dentate gyrus volume.

204

205For GABAergic boutons an optical fractionator protocol was developed and validated using rat
206hippocampi to ensure accuracy (Table 1). For rats the number of stereologically estimated immuno-
207labeled gephyrin punctae and electron microscopically identified GABA-immunopositive synapses have
208been reported (Thind et al., 2010). Experiments were approved by the Stanford University Institutional
209Animal Care and Use Committee and conducted in compliance with the U.S. National Research
210Council's "Guide for the Care and Use of Laboratory Animals" the U.S. Public Health Service's "Policy

211on Humane Care and Use of Laboratory Animals” and “Guide for the Care and Use of Laboratory
212Animals.” In the present study, Sprague-Dawley rats, 2 females, 2 males, 7 months old, were
213euthanized with pentobarbital (>100 mg/kg intraperitoneally) and perfused through the ascending aorta
214(30 ml/min) for 1 min with 0.9% NaCl and 30 min with 4% formaldehyde in PB. At 4°C brains post-fixed
215overnight then equilibrated in 30% sucrose in PB. Hippocampi were dissected from the brain,
216straightened, frozen, and sectioned from the septal pole to the temporal pole with a sliding microtome
217set at 40 μ m. Starting at a random point near the septal pole, a 1-in-24 series of sections was sampled
218and processed with a staining protocol optimized to label GABAergic synaptic boutons in rat tissue
219(Figure 2), using the same antibodies as for sea lions: one to GAD65/67 (1:60,000, L127/12, UC
220Davis/NIH NeuroMab Facility) and the other to VGAT (1:3000, MSFR106160, Frontier Institute), but
221preceded by antigen retrieval in 0.5 M citrate buffer with 1% NaCl (pH 8.6) at 90°C for 70 min, and
222avidin/biotin blocking. Additionally, triton was omitted necessitating room temperature incubations for
223penetration, which required 0.1% sodium azide in the primary solution.

224

225To estimate the number of GABAergic boutons, Stereo Investigator was used to draw contours around
226the granule cell layer, inner third of the molecular layer, middle third, and outer third. Each layer was
227analyzed separately. The molecular layer is where dendrites receive 91% of a granule cell’s total
228GABAergic synaptic input (Halasy and Somogyi, 1993). The hilus was not analyzed. At each sample
229site a stack of images was collected at 1 μ m depth intervals using a 63X Plan-Apochromat 1.4 na lens
230(Zeiss) and a color camera (1" CMOS sensor, 3216 x 2208). Images were digitally zoomed. Section
231thickness was measured. Boutons were counted if they appeared in focus for the first time in a 1 μ m
232thick disector. This analysis revealed that the estimated number of boutons per dentate gyrus was
233 $1.79 \pm 0.88 \times 10^9$ (mean \pm standard error of mean, range, $1.54 - 1.94 \times 10^9$), which was comparable but
234less than the reported number of gephyrin-positive punctae (1.99×10^9) and GABA-positive synapses
235(3.3×10^9) in control rats (Thind et al., 2010). A single GABAergic bouton in the rat dentate gyrus can
236make multiple synapses (Buckmaster et al., 2016), so the number of boutons would be expected to be
237less than the number of synapses. The distribution of boutons across layers of the rat dentate gyrus:

2380.19 ± 0.06 (mean ± 95% confidence interval of mean) in the granule cell layer, 0.15 ± 0.03 in the inner
239molecular layer, 0.23 ± 0.02 in the middle molecular layer, and 0.43 ± 0.02 in the outer molecular layer
240($p < 0.001$, ANOVA with Holm-Sidak method) was similar to the distribution of gephyrin punctae and
241GABAergic synapses. The same optical fractionator protocol was used to estimate numbers of
242GABAergic boutons in sea lions, except the counting grid was larger because sea lion sections were
243larger. The mean coefficient of error of the stereological analysis was consistently less than the
244coefficient of variation, indicating sufficient within animal sampling (Table 1; West et al., 1991).

245

246 Statistics

247 There are 4 hippocampal groups: controls, bilateral sclerotics, unilateral sclerotics, and unilateral non-
248 sclerotics. Unilateral non-sclerotics are an instructive within-animal control for unilateral sclerotics.
249 Results were analyzed by unpaired two-tailed t tests, ANOVA, and Pearson Product Moment
250 Correlation (Systat). Assumptions of normality and equal variance were checked. If verification failed,
251 Mann-Whitney rank sum test or Kruskal-Wallis ANOVA on ranks was used. If differences among
252 groups were greater than would be expected by chance ($p < 0.05$), the Holm-Sidak or Dunn's method
253 was used to isolate the group or groups that differed from the others.

254

255 Results

256 Dentate gyrus volume

257 The average volume of the dentate gyrus was similarly large in control (92 mm³) and unilateral non-
258 sclerotic hippocampi (106 mm³, Figure 3A, Table 2). Unilateral sclerotic hippocampi had an average
259 dentate gyrus volume of 48 mm³ which was 45% of unilateral non-sclerotic hippocampi ($p < 0.001$,
260 ANOVA). Comparably, bilateral sclerotic hippocampi had an average dentate gyrus volume of 54 mm³
261 which was 59% of control hippocampi ($p < 0.001$). Overall, the average volume of the dentate gyrus in
262 control and unilateral non-sclerotic hippocampi was 97 mm³. In sclerotics the average volume of the
263 dentate gyrus was 51 mm³ (47% smaller, $p < 0.0001$, t test).

264

265 Granule cells

266 As reported previously, the average number of granule cells per dentate gyrus was similar in control
267 (2.32 million) and unilateral non-sclerotic hippocampi (2.38 million, Figure 3B, Table 2). Nissl stained
268 sections used to estimate granule cell numbers also revealed severe hilar neuron loss that was a
269 defining feature of sclerotic hippocampi (Figures 4D, 6D). Unilateral sclerotic hippocampi had an
270 average of 0.63 million granule cells, which was 26% of unilateral non-sclerotic hippocampi ($p < 0.001$,
271 ANOVA). Similarly, bilateral sclerotic hippocampi had an average of 0.46 million granule cells, which
272 was 20% of control hippocampi ($p < 0.001$). Overall, the average number of granule cells in control and
273 unilateral non-sclerotic hippocampi was 2.33 million. In sclerotics it was 0.52 million (78% fewer,
274 $p < 0.0001$, t test).

275

276 GAD cells

277 The average number of GAD cells per dentate gyrus was similar in control (244,400) and unilateral
278 non-sclerotic hippocampi (230,100, Figures 3C and 4, Table 2). Sclerotic hippocampi demonstrated
279 considerable loss of GAD cells. Bilateral sclerotic hippocampi had an average of 87,400 GAD neurons,
280 which was 36% of control hippocampi ($p < 0.001$, ANOVA). Unilateral sclerotic hippocampi had only
281 145,700 GAD neurons, which was 20% of unilateral non-sclerotic hippocampi ($p < 0.001$). Overall, the
282 average number of GAD cells in control and unilateral non-sclerotic hippocampi was 239,000. In
283 sclerotic hippocampi it was 66,600 (72% loss, $p < 0.0001$, t test). These findings reveal substantial loss
284 of GAD cells in the dentate gyrus of sclerotic hippocampi.

285

286 GAD cells were distributed across all layers of the dentate gyrus (Figure 4). To evaluate GAD cell
287 distribution between dentate gyrus compartments, data from control and unilateral non-sclerotic
288 hippocampi were combined and compared to that of bilateral and unilateral sclerotic hippocampi
289 combined. Left and right hippocampi from control and bilateral hippocampi were averaged yielding a
290 single value per section. In control and non-sclerotic hippocampi on average 50% of the GAD cell
291 profiles were in the hilus, 20% were in the granule cell layer, and 30% were in the molecular layer

292(Figure 5AB). In sclerotic hippocampi there were fewer GAD cell profiles in all layers of the dentate
293gyrus ($p < 0.0001$, t tests). Proportionally, compared to non-sclerotics, sclerotic hippocampi had fewer
294GAD cells in the hilus ($p = 0.002$, Mann-Whitney rank sum test) and more in the granule cell layer
295($p = 0.045$). These findings suggest GAD cell loss in sclerotic hippocampi was most severe in the hilus of
296the dentate gyrus. The proportional loss of GAD cells in sclerotic hippocampi was similar at all
297septotemporal levels of the hippocampus (Figure 5C).

298

299GABAergic boutons

300The average number of GABAergic synaptic boutons per dentate gyrus was high in control (5.67×10^9)
301and unilateral non-sclerotic sea lion hippocampi (6.90×10^9) and low in unilateral sclerotic (2.58×10^9)
302and bilateral sclerotic hippocampi (1.84×10^9 , $p < 0.001$, Kruskal-Wallis ANOVA on ranks, Figure 3D and
303Figure 6, Table 2). The average number of GABAergic boutons in unilateral sclerotic hippocampi was
30437% of unilateral non-sclerotic hippocampi ($p < 0.05$). The average number of GABAergic boutons in
305bilateral sclerotic hippocampi was 33% of controls ($p < 0.05$). Overall, the average number of boutons in
306control and unilateral non-sclerotic hippocampi was 5.96×10^9 . In sclerotics it was 2.09×10^9 (65%
307fewer, $p < 0.0001$, t test). These findings reveal extensive loss of GABAergic synaptic boutons in
308sclerotic hippocampi. However, in the sclerotic group the average loss of GABAergic boutons (65%
309fewer) was not greater than the average loss of granule cells (78% fewer), which is evidence against
310the hypothesis that bouton loss is disproportionately more severe than granule cell loss in temporal lobe
311epilepsy.

312

313In sclerotic hippocampi, loss of GABAergic boutons occurred in the granule cell layer, inner molecular
314layer, middle molecular layer, and outer molecular layer (Figure 7A). The pattern of bouton distribution
315across layers of the dentate gyrus was similar in control and non-sclerotic versus sclerotic hippocampi
316(Figure 7B). Proportionally the fewest boutons were in the granule cell layer (0.14-0.17), then inner
317molecular layer (0.19-0.21), then middle molecular layer (0.27-0.30), and most were in the outer
318molecular layer (0.34-0.37) ($p < 0.001$, ANOVA with Holm-Sidak method). In sclerotic hippocampi of sea

319lions, loss of boutons was distributed relatively proportionally along the septotemporal axis of the
320hippocampus (Figure 7C).

321

322Correlation testing

323Results of the present study revealed smaller volumes of the dentate gyrus, fewer granule cells, fewer
324GAD cells, and fewer GABAergic boutons in sclerotic hippocampi. To determine if any of these
325pathological changes were associated with others, correlation testing was performed. In sclerotic
326hippocampi, there were no significant correlations with the number of GAD cells and dentate gyrus
327volume ($r=0.11$, $p=0.60$, Pearson Moment Correlation), the number of GAD cells and number of granule
328cells ($r=-0.19$, $p=0.38$), or the number of GAD cells and the number of GABAergic boutons ($r=-0.22$,
329 $p=0.29$).

330

331There was a significant correlation between dentate gyrus volume and the number of granule cells in
332sclerotic hippocampi ($r=0.56$, $p=0.005$, Pearson Moment Correlation) and in all hippocampi: sclerotic
333plus non-sclerotic ($r=0.88$, $p<0.0001$, Figure 8A). Similarly, there was a significant correlation between
334dentate gyrus volume and the number of GABAergic boutons in sclerotic ($r=0.68$, $p=0.0003$) and all
335hippocampi ($r=0.85$, $p<0.0001$, Figure 8B).

336

337Notably, there was a significant correlation between the number of GABAergic boutons and the number
338of granule cells in sclerotic ($r=0.68$, $p=0.0002$, Pearson Moment Correlation) and all hippocampi
339($r=0.79$, $p<0.0001$, Figure 8C). This is important as it pertains to the hypothesis being tested. If there
340had been disproportionate loss of GABAergic boutons in sclerotic hippocampi, as the hypothesis
341contends, then in the group of sclerotic hippocampi, as the number of granule cells decreased, the
342number of GABAergic boutons would have declined at a faster rate than in the non-sclerotic group. A
343regression line through the sclerotic hippocampal group would have had a steeper slope than a
344regression line for non-sclerotic hippocampi. On the contrary, the slope of a regression line through the
345sclerotic group (1530 boutons per granule cell) was slightly less, not greater, than the slope of a
346regression line through the non-sclerotic group (1740 boutons per granule cell). These findings do not

347support the hypothesis of disproportionate loss of GABAergic boutons relative to granule cells in
348sclerotic hippocampi.

349

350**Discussion**

351The principal findings of this study are that sea lions with sclerotic hippocampi and temporal lobe
352epilepsy have a smaller dentate gyrus with fewer granule cells, fewer GAD cells, and fewer GABAergic
353boutons. Importantly, the number of granule cells and GABAergic boutons are significantly correlated in
354sclerotic hippocampi, and the loss of boutons is not more severe than the loss of granule cells.

355

356**Motivation**

357The present study sought to test the hypothesis that in temporal lobe epilepsy there is a
358disproportionate loss of GABAergic boutons relative to granule cells. Challenges of anatomical
359research on human patients constrained important and interesting previous human studies (Babb et al.,
3601989; Wittner et al., 2001; Wittner and Maglóczy, 2017; Alhourani et al., 2020). Sea lions with naturally
361occurring temporal lobe epilepsy address some limitations of human studies by providing larger sample
362sizes, superior controls, tissue perfused with fixative immediately after euthanasia, and stereological
363evaluation of bilateral dentate gyri in their entirety. Another notable improvement is analysis of both
364somatic and dendritic domains, not just the granule cell layer.

365

366**Dentate gyrus volume and granule cells**

367The volume of the dentate gyrus in sclerotic hippocampi of epileptic sea lions was approximately half
368the size of a control. This is similar to the shrinkage of entire hippocampi that was found in sea lions
369using magnetic resonance imaging (Montie et al., 2010). Dentate gyrus shrinkage correlates with
370granule cell loss, which is severe in sea lions. In sclerotic hippocampi of human patients there is an
371average of 50% loss of granule cells (Babb et al., 1989; Kim et al., 1990; Sass et al., 1990; Mathern et
372al., 1995, 1996; de Lanerolle et al., 2003; Thom et al., 2005; Blümcke et al., 2007). In contrast, granule
373cells are generally preserved in epileptic rodents (Thind et al., 2010; Buckmaster and Lew, 2011), and

374while there are some reports of reduced granule cell density in chronic rodent models (Mello et al.,
3751993; Cavazos et al., 1994; Mathern et al., 1997; Mathern and Bertram, 2012), they do not approach
376the reductions in sea lions or humans.

377

378GAD cells

379GAD cell loss was substantial in epileptic sea lions with sclerotic hippocampi. Loss of GAD cells raises
380the possibility that granule cells lose inhibitory synaptic input, become hyperexcitable, and cause
381seizures. Like epileptic sea lions, rat models of temporal lobe epilepsy display GAD cell loss in the
382dentate gyrus (Obenaus et al., 1993; Houser and Esclapez, 1996; Buckmaster and Jongen-Rêlo,
3831999). In contrast, preservation of GAD cells in the dentate gyrus of patients with temporal lobe
384epilepsy has been reported (Babb et al., 1989; Mathern et al., 1995). The difference might be
385attributable to cell counting methods (density measures versus stereology, given granule cell
386dispersion), sensitivity of GAD antibodies, tissue processing protocols, and/or quality or type of control
387tissue. Previous studies of the dentate gyrus in sclerotic hippocampi in patients with temporal lobe
388epilepsy used antibodies for markers of various cell types and found interneuron loss (Sloviter et al.,
3891991; Zhu et al., 1997; Maglóczy et al., 2000; Andrioli et al., 2007; Tóth et al., 2010), including
390somatostatin cells (de Lanerolle et al., 1989; Mathern et al., 1995). In sea lions, somatostatin cell loss
391(Buckmaster et al., 2014) could be an important contributor to GAD cell loss, which was most severe in
392the hilus.

393

394GABAergic boutons

395GABAergic bouton numbers were severely reduced in the dentate gyrus of sea lions with temporal lobe
396epilepsy. In a number of different rodent models of chronic temporal lobe epilepsy following an initial
397decrease in the first week after status epilepticus there is an increase in the labeling of GABAergic
398boutons in the inner, outer, or entire molecular layer (Davenport et al., 1990; Houser and Esclapez,
3991996; Mathern et al., 1997; Esclapez and Houser, 1999; Andre et al., 2001), which was stereologically
400quantified by Thind et al. (2010). In dentate gyrus resected from humans with temporal lobe epilepsy

401the number of GABAergic boutons and synapses per granule cell, or their density, are increased in the
402granule cell layer (Babb et al., 1989; Wittner et al., 2001; Wittner and Maglóczy, 2017; Alhourani et al.,
4032020). These findings from patients and rodents suggest that GABAergic synapses with granule cells
404are increased, not reduced, in temporal lobe epilepsy. Given that the loss of granule cells was more
405severe than the loss of GABAergic boutons in epileptic sea lions, results of the present study are
406consistent with more GABAergic boutons per granule cell in epileptic patients and rodent models.

407

408Numbers of GABAergic boutons and granule cells were correlated in sclerotic hippocampi of sea lions.
409It is unclear whether the correlation was present immediately after the precipitating injury or if axon
410sprouting resulted in the correlation. If there were GABAergic axon sprouting it could come from local
411(Zhang et al., 2009; Peng et al., 2013) or extrahippocampal (Soussi et al., 2014) GAD cells. While
412GABAergic bouton loss was correlated with granule cell loss, it was not correlated with GAD cell loss.
413These findings suggest that following a precipitating injury, if GABAergic axon sprouting occurs, then it
414might be influenced more by the availability of granule cell synaptic targets than by the number of GAD
415cells in the dentate gyrus.

416

417Limitations

418Limitations of the present study include those of the sea lion model that have been discussed
419(Buckmaster, 2017). Immunolabeling GAD cells can be challenging (Obenaus et al., 1993; Houser and
420Esclapez, 1996). Attempts to use in situ hybridization on sea lion tissue were unsuccessful, but after
421protocols were optimized, GAD immunostaining revealed well-labeled cells at numbers proportionally
422appropriate compared to rats processed with in situ hybridization for GAD (Buckmaster and Jongen-
423Rêlo, 1999; Thind et al., 2010). Quantifying synaptic boutons was challenging. Boutons are small,
424densely packed, and sometimes overlapping in sections. A new camera and lens were used to better
425visualize boutons, and a new optical fractionator protocol was developed that generated stacked and
426zoomed images. The new methods yielded results from rat tissue consistent with a previous rat study
427that used confocal and electron microscopic approaches to label and quantify GABAergic synapses

428(Thind et al., 2010). Results from control sea lion tissue were proportionally appropriate compared to
429bouton results of rats in the present study. Sea lion GABAergic synaptic bouton counts in the present
430study suggest previous analyses of parvalbumin- (Cameron et al., 2018) and cannabinoid receptor 1-
431labeled boutons in sea lions (Seelman et al., 2022) that were analyzed with other methods might have
432been underestimated. However, the relative comparisons of control and epileptic groups should be valid
433as all groups were evaluated with identical techniques in those studies.

434

435While the present study quantified GABAergic bouton numbers in the granule cell and molecular layers
436of the dentate gyrus, how many synapses each bouton made, and which cell types they targeted was
437not certain. Adding to the uncertainty, reorganization of synaptic input to granule cells (Du et al., 2017)
438and interneurons (Sloviter et al., 2012) is reported in rodent models of temporal lobe epilepsy. Besides
439granule cells, potential synaptic targets include interneurons in the molecular and granule cell layers,
440and dendrites from some hilar interneurons and mossy cells that extend into the molecular layer.
441However, many hilar GAD cell and mossy cell dendrites remain confined to the hilus and do not extend
442into the granule cell and molecular layers. Furthermore, hilar neuron numbers are substantially reduced
443in sea lions with sclerotic hippocampi (Buckmaster et al., 2014). For a conservative quantitative
444estimate, potential non-granule cell targets can be overestimated by assuming that all surviving hilar
445neurons (quantified in the 2014 study) and interneurons were synaptic targets. Even then, sclerotic
446hippocampi would be estimated to have over five times more granule cells than all other potential target
447neurons combined. Thus, granule cells remained the most abundant synaptic target of GABAergic
448boutons in the granule cell and molecular layers of sclerotic hippocampi.

449

450Conclusion

451Data of the present study show that numbers of granule cells and GABAergic boutons were reduced
452and correlated in sclerotic hippocampi. Other sea lion studies that used interneuron subtype specific
453markers find no disproportionate loss of GABAergic boutons (Cameron et al., 2019; Seelman et al.,
4542022). Similarly, studies of human patients with temporal lobe epilepsy and rodent models report no

455 disproportionate loss of GABAergic boutons or inhibitory synapses (Babb et al., 1989; Wittner et al.,
456 2001; Thind et al., 2010; Wittner and Maglóczy, 2017; Alhourani et al., 2020). On the contrary, they
457 report more boutons per granule cell. Together, these findings contradict the hypothesis that
458 disproportionate reductions in GABAergic boutons and synapses reduces inhibition of granule cells.
459 What then reduces inhibition of granule cells in patients and animal models of temporal lobe epilepsy
460 (see Introduction)? If in epileptic hippocampi GABAergic boutons are in place at sufficient numbers but
461 dysfunctional (Zhang and Buckmaster, 2009), it might be possible to reestablish synaptic function and
462 provide seizure relief.

463

464

465

466

467

468

469

470

471

472

473

474

475

eNeuro Accepted Manuscript

476References

- 477Adel SS, Clarke VRJ, Evans-Strong A, Maguire J, Paradis S (2023) Semaphorin 4D induced inhibitory
478 synaptogenesis decreases epileptiform activity and alters progression to status epilepticus in mice.
479 *Epilepsy Res* 193:107156.
- 480Alhourani A, Rish KN, Wozny TA, Sudhakar V, Hamilton RL, Richardson RM (2020) GABA bouton
481 subpopulations in the human dentate gyrus are differentially altered in mesial temporal lobe epilepsy.
482 *J Neurophysiol* 123:392-406.
- 483André V, Marescaux C, Nehlig A, Fritschy JM (2001) Alterations of hippocampal GABAergic system
484 contribute to development of spontaneous recurrent seizures in the rat lithium-pilocarpine model of
485 temporal lobe epilepsy. *Hippocampus* 11:452-468.
- 486Andrioli A, Alonso-Nanclares L, Arellano JI, DeFelipe J (2007) Quantitative analysis of parvalbumin-
487 immunoreactive cells in the human epileptic hippocampus. *Neuroscience* 149:131-143.
- 488Babb TL, Pretorius JK, Kupfer WR, Crandall PH (1989) Glutamate decarboxylase-immunoreactive
489 neurons are preserved in human epileptic hippocampus. *J Neurosci* 9:2562-2574.
- 490Blümcke I, Pauli E, Clusmann H, Schramm J, Becker A, Elger C, Merschhemke M, Meencke HJ,
491 Lehmann T, von Deimling A, Scheiwe C, Zentner J, Volk B, Romstöck J, Stefan H, Hildebrandt M
492 (2007) A new clinico-pathological classification system for mesial temporal sclerosis. *Acta*
493 *Neuropathol* 113:235-244.
- 494Boulland JL, Ferhat L, Solbu TT, Ferrand N, Chaudhry FA, Storm-Mathisen J, Esclapez M (2007)
495 Changes in vesicular transporters for γ -aminobutyric acid and glutamate reveal vulnerability and
496 reorganization of hippocampal neurons following pilocarpine-induced seizures. *J Comp Neurol*
497 503:466-485.
- 498Buckmaster PS (2017) Naturally occurring epilepsy and status epilepticus in sea lions. In: *Models of*
499 *Seizure and Epilepsy*, Second Edition, Pitkänen A, Buckmaster PS, Galanopoulou AS, Moshe SM,
500 eds, Elsevier, New York. pp 413-425.
- 501Buckmaster PS, Jongen-Rêlo AL (1999) Highly specific neuron loss preserves lateral inhibitory circuits
502 in the dentate gyrus of kainate-induced epileptic rats. *J Neurosci* 19:9519-9529.

503 Buckmaster PS, Lew FH (2011) Rapamycin suppresses mossy fiber sprouting but not seizure
504 frequency in a mouse model of temporal lobe epilepsy. *J Neurosci* 31:2337-2347.

505 Buckmaster PS, Wen X, Toyoda I, Gulland FMD, Van Bonn W (2014) Hippocampal neuropathology of
506 domoic acid-induced epilepsy in sea lions (*Zalophus californianus*). *J Comp Neurol* 522:1691-1706.

507 Buckmaster PS, Yamawaki R, Thind K (2016) More docked vesicles and larger active zones at basket
508 cell-to-granule cell synapses in a rat model of temporal lobe epilepsy. *J Neurosci* 36:3295-3308.

509 Cameron S, Lopez A, Glabman R, Abrams E, Johnson S, Field C, Gulland FMD, Buckmaster PS
510 (2019) Proportional loss of parvalbumin-immunoreactive synaptic boutons and granule cells from the
511 hippocampus of sea lions with temporal lobe epilepsy. *J Comp Neurol* 527:2341-2355.

512 Casalia ML, Howard MA, Baraban SC (2017) Persistent seizure control in epileptic mice transplanted
513 with gamma-aminobutyric acid progenitors. *Ann Neurol* 82:530-542.

514 Cavazos JE, Das I, Sutula TP (1994) Neuronal loss induced in limbic pathways by kindling: evidence
515 for induction of hippocampal sclerosis by repeated brief seizures. *J Neurosci* 14:3106-3121.

516 Chaudhry FA, Reimer RJ, Bellocchio EE, Danbolt NC, Osen KK, Edwards RH, Storm-Mathisen (1998)
517 The vesicular GABA transporter, VGAT, localizes to synaptic vesicles in sets of glycinergic as well as
518 GABAergic neurons. *J Neurosci* 18:9733-9750.

519 Davenport CJ, Brown WJ, Babb TL (1990) Sprouting of GABAergic and mossy fiber axons in dentate
520 gyrus following intrahippocampal kainate in the rat. *Exp Neurol* 109:180-190.

521 de Lanerolle NC, Kim JH, Robbins RJ, Spencer DD (1989) Hippocampal interneuron loss and plasticity
522 in human temporal lobe epilepsy. *Brain Res* 495:387-395.

523 de Lanerolle NC, Kim JH, Williamson A, Spencer SS, Zaveri HP, Eid T, Spencer DD (2003) A
524 retrospective analysis of hippocampal pathology in human temporal lobe epilepsy: evidence for
525 distinctive patient subcategories. *Epilepsia* 44:677-687.

526 Dengler CG, Yue C, Takano H, Coulter DA (2017) Massively augmented hippocampal dentate granule
527 cell activation accompanies epilepsy development. *Sci Rep* 7:42090.

528 Du X, Zhang H, Parent JM (2017) Rabies tracing of birthdated dentate granule cells in rat temporal lobe
529 epilepsy. *Ann Neurol* 81:790-803.

530 Duckrow RB, Spencer SS (1992) Regional coherence and the transfer of ictal activity during seizure
531 onset in the medial temporal lobe. *Electroencephalogr Clin Neurophysiol* 82:415-422.

532 Engel J Jr, Williamson PD, Wieser H (1997) Mesial temporal lobe epilepsy. In: Engel J Jr, Pedley TA,
533 eds. *Epilepsy: A Comprehensive Textbook*. Philadelphia: Lippincott-Raven Press. pp 2417-2426.

534 Esclapez M, Houser CR (1999) Up-regulation of GAD65 and GAD67 in remaining hippocampal GABA
535 neurons in a model of temporal lobe epilepsy. *J Comp Neurol* 412:488-505.

536 Fong AY, Stometta RL, Foley CM, Potts JT (2005) Immunohistochemical localization of GAD67-
537 expressing neurons and processes in the rat brainstem: subregional distribution in the nucleus tractus
538 solitarius. *J Comp Neurol* 493:274-290.

539 Franck JE, Pokorny J, Kunkel DD, Schwartzkroin PA (1995) Physiologic and morphologic
540 characteristics of granule cell circuitry in human epileptic hippocampus. *Epilepsia* 36:543-558.

541 Fujihara K, Yamada K, Ichitani Y, Kakizaki T, Jiang W, Miyata S, Suto T, Saito S, Watanabe M, Kajita
542 Y, Ohshiro T, Mushiake H, Miyasaka Y, Mashimo T, Yasuda H, Yanagawa Y (2020) CRISPER/Cas9-
543 engineered Gad1 elimination in rats leads to complex behavioral changes: implications for
544 schizophrenia. *Transl Psychiatry* 10:426-439.

545 Fukuda T, Aika Y, Heizmann CW, Kosaka T (1998) GABAergic axon terminals at perisomatic and
546 dendritic inhibitory sites show different immunoreactivities against two GAD isoforms, GAD67 and
547 GAD65, in the mouse hippocampus: a digitized quantitative analysis. *J Comp Neurol* 395:177-194.

548 Fukudome Y, Ohno-Shosaku T, Matsui M, Omori Y, Fukaya M, Tsubokawa H, Taketo MM, Watanabe
549 M, Manabe T, Kano M (2004) Two distinct classes of muscarinic action on hippocampal inhibitory
550 synapses: M2-mediated direct suppression and M1/M3-mediated indirect suppression through
551 endocannabinoid signaling. *Eur J Neurosci* 19:2682-2692.

552 Gabriel S, Njunting M, Pomper JK, Merschhemke M, Sanabria ER, Eilers A, Kivi A, Zeller M, Meencke
553 HJ, Cavalheiro EA, Heinemann U, Lehmann TN (2004) Stimulus and potassium-induced epileptiform
554 activity in the human dentate gyrus from patients with and without hippocampal sclerosis. *J Neurosci*
555 24:10416-10430.

556 Greenfield Jr LJ (2013) Molecular mechanisms of antiseizure drug activity at GABA_A receptors. *Seizure*
557 22:589-600.

558 Halasy K, Somogyi P (1993) Distribution of GABAergic synapses and their targets in the dentate gyrus
559 of rat: a quantitative immunoelectron microscopic analysis. *J Hirnforsch* 34:299-308.

560 Heinemann U, Beck H, Dreier JP, Ficker E, Stabel J, Zhang CL (1992) The dentate gyrus as a
561 regulated gate for the propagation of epileptiform activity. *Epilepsy Res Suppl* 7:273-280.

562 Hesdorffer DC, Logroscino G, Benn EK, Katri N, Cascino G, Hauser WA (2011) Estimating risk for
563 developing epilepsy. *Neurology* 76:23-27.

564 Houser CR, Esclapez M (1994) Localization of mRNAs encoding two forms of glutamic acid
565 decarboxylase in the rat hippocampal formation. *Hippocampus* 4:530-545.

566 Houser CR, Esclapez M (1996) Vulnerability and plasticity of the GABA system in the pilocarpine model
567 of spontaneous recurrent seizures. *Epilepsy Res* 26:207-218.

568 Hunt RF, Girkis KM, Rubenstein JL, Alvarez-Buylla A, Baraban SC (2013) GABA progenitors grafted
569 into the adult epileptic brain control seizures and abnormal behavior. *Nat Neurosci* 16:692-697.

570 Isokawa M (1996) Decrement of GABA_A receptor-mediated inhibitory postsynaptic currents in dentate
571 granule cells in epileptic hippocampus. *J Neurophysiol* 75:1901-1908.

572 Isokawa M, Avanzini G, Finch DM, Babb TL, Levesque MF (1991) Physiologic properties of human
573 dentate granule cells in slices prepared from epileptic patients. *Epilepsy Res* 9:242-250.

574 Isokawa M, Levesque MF (1991) Increased NMDA responses and dendritic degeneration in human
575 epileptic hippocampal neurons in slices. *Neurosci Lett* 132:212-216.

576 Jandová K, Päsler D, Antonio LL, Raue C, Ji S, Njunting M, Kann O, Kovács R, Meencke H, Cavalheiro
577 EA, Heinemann U, Gabriel S, Lehmann T (2006) Carbamazepine-resistance in the epileptic dentate
578 gyrus of human hippocampal slices. *Brain* 129:3290-3306.

579 Kim JH, Guimaraes PO, Shen MY, Masukawa LM, Spencer DD (1990) Hippocampal neuronal density
580 in temporal lobe epilepsy with and without gliomas. *Acta Neuropathol* 80:41-45.

581 King D, Bronen RA, Spencer DD, Spencer SS (1997) Topographic distribution of seizure onset and
582 hippocampal atrophy: relationship between MRI and depth EEG. *Electroencephalogr Clin*
583 *Neurophysiol* 103:692-697.

584 Kobayashi M, Buckmaster PS (2003) Reduced inhibition of dentate granule cells in a model of temporal
585 lobe epilepsy. *J Neurosci* 23:2440-2452.

586 Krook-Magnuson E, Armstrong C, Bui A, Lew S, Oijala M, Soltesz I (2015) In vivo evaluation of the
587 dentate gate theory in epilepsy. *J Physiol* 593:2379-2388.

588 Lothman EW, Bertram 3rd EH, Stringer JL (1991) Functional anatomy of hippocampal seizures. *Prog*
589 *Neurobiol* 37:1-82.

590 Maglóczy Z, Wittner L, Borhegyi Z, Halász P, Vajda J, Czirják S, Freund TF (2000) Changes in the
591 distribution and connectivity of interneurons in the epileptic human dentate gyrus. *Neuroscience* 96:7-
592 25.

593 Margerison JH, Corsellis JA (1966) Epilepsy and the temporal lobes. *Brain* 89:499-530.

594 Masukawa LM, Higashima M, Kim JH, Spencer DD (1989) Epileptiform discharges evoked in
595 hippocampal brain slices from epileptic patients. *Brain Res* 493:168-174.

596 Masukawa LM, O'Connor WM, Lynott J, Burdette LJ, Uruno K, McGonigle P, O'Connor MJ (1995)
597 Longitudinal variation in cell density and mossy fiber reorganization in the dentate gyrus from
598 temporal lobe epileptic patients. *Brain Res* 678:65-75.

599 Mathern GW, Babb TL, Pretorius JK, Leite JP (1995) Reactive synaptogenesis and neuron densities for
600 neuropeptide Y, somatostatin, and glutamate decarboxylase immunoreactivity in the epileptogenic
601 human fascia dentata. *J Neurosci* 15:3990-4004.

602 Mathern GW, Babb TL, Leite JP, Pretorius K, Yeoman KM, Kuhlman PA (1996) The pathogenic and
603 progressive features of chronic human hippocampal epilepsy. *Epilepsy Res* 26:151-161.

604 Mathern GW, Bertram EH 3rd, Babb TL, Pretorius JK, Kuhlman PA, Spradlin S, Mendoza D (1997) In
605 contrast to kindled seizures, the frequency of spontaneous epilepsy in the limbic status model
606 correlates with greater aberrant fascia dentata excitatory and inhibitory axon sprouting, and increased
607 staining for N-methyl-D-aspartate, AMPA and GABA(A) receptors. *Neuroscience* 77:1003-1019

608 Mathern GW, Bertram EH 3rd (2021) Recurrent limbic seizures do not cause hippocampal neuronal
609 loss: A prolonged laboratory study. *Neurobiol Dis* 148:105183.

610 Mello LE, Cavalheiro EA, Tan AM, Kupfer WR, Pretorius JK, Babb TL, Finch DM (1993) Circuit
611 mechanisms of seizures in the pilocarpine model of chronic epilepsy: cell loss and mossy fiber
612 sprouting. *Epilepsia* 34:985-995.

613 Montie EW, Wheeler E, Pussini N, Battey TW, Barakos J, Dennison S, Colegrove K, Gulland F (2010)
614 Magnetic resonance imaging quality and volumes of brain structures from live and postmortem
615 imaging of California sea lions with clinical signs of domoic acid toxicosis. *Dis Aquat Organ* 91:243-
616 256.

617 Obenaus A, Esclapez M, Houser CR (1993) Loss of glutamate decarboxylase mRNA-containing
618 neurons in the rat dentate gyrus following pilocarpine-induced seizures. *J Neurosci* 13:4470-4485.

619 Pathak HR, Weissinger F, Terunuma M, Carlson GC, Hsu F, Moss SJ, Coulter DA (2007) Disrupted
620 dentate granule cell chloride regulation enhances synaptic excitability during development of temporal
621 lobe epilepsy. *J Neurosci* 27:14012-14022.

622 Peng Z, Zhang N, Wei W, Huang C, Cetina Y, Otis TS, Houser CR (2013) A reorganized GABAergic
623 circuit in a model of epilepsy: evidence from optogenetic labeling and stimulation of somatostatin
624 interneurons. *J Neurosci* 33:14392-14405.

625 Quesney LF (1986) Clinical and EEG features of complex partial seizures of temporal lobe origin.
626 *Epilepsia* 27(Suppl 2): S27-S45.

627 Ribak CE, Vaughn JE, Siato K (1978) Immunocytochemical localization of glutamic acid decarboxylase
628 in neuronal somata following colchicine inhibition of axonal transport. *Brain Res* 140:315-332.

629 Sass KJ, Spencer DD, Kim JH, Westerveld M, Novelly RA, Lencz T (1990) Verbal memory impairment
630 correlates with hippocampal pyramidal cell density. *Neurology* 40:1694-1697.

631 Sayin U, Osting S, Hagen J, Rutecki P, Sutula T (2003) Spontaneous seizures and loss of axo-axonic
632 and axo-somatic inhibition induced by repeated brief seizures in kindled rats. *J Neurosci* 23:2759-
633 2768.

634 Seelman A, Vu K, Buckmaster P, Field C, Johnson S, Mackie K, Wyeth M (2022) Cannabinoid receptor
635 1-labeled boutons in the sclerotic dentate gyrus of epileptic sea lions. *Epilepsy Res* 184:106965.

636 Shao LR, Dudek FE (2005) Changes in mIPSCs and sIPSCs after kainate treatment: evidence for loss
637 of inhibitory input to dentate granule cells and possible compensatory responses. *J Neurophysiol*
638 94:952-960.

639 Sloviter RS, Bumanglag AV, Schwarcz R, Frotscher M (2012) Abnormal dentate gyrus network circuitry
640 in temporal lobe epilepsy. In: Noebels JL, Avoli M, Rogawski MA, Olsen RW, Delgado-Escueta AV,
641 eds. *Jasper's Basic Mechanisms of the Epilepsies*, Fourth Edition. New York: Oxford University
642 Press. pp 454-469.

643 Sloviter RS, Sollas AL, Barbaro NM, Laxer KD (1991) Calcium-binding protein (calbindin-D28K) and
644 parvalbumin immunocytochemistry in the normal and epileptic human hippocampus. *J Comp Neurol*
645 308:381-396.

646 Soussi R, Boulland JL, Bassot E, Bras H, Coulon P, Chaudhry FA, Storm-Mathisen J, Ferhat L,
647 Esclapez M (2015) Reorganization of supramammillary-hippocampal pathways in the rat pilocarpine
648 model of temporal lobe epilepsy: evidence for axon terminal sprouting. *Brain Struct Funct* 220:2449-
649 2468.

650 Spencer SS, Spencer DD (1994) Entorhinal-hippocampal interactions in medial temporal lobe epilepsy.
651 *Epilepsia* 35:721-727.

652 Spencer SS, Williamson PD, Spencer DD, Mattson RH (1987) Human hippocampal seizure spread
653 studied by depth and subdural recording: the hippocampal commissure. *Epilepsia* 28:479-489.

654 Spencer SS, Spencer DD, Williamson PD, Mattson R (1990) Combined depth and subdural electrode
655 investigation in uncontrolled epilepsy. *Neurology* 40:74-79.

656 Sperling MR, O'Connor MJ (1989) Comparison of depth and subdural electrodes in recording temporal
657 lobe seizures. *Neurology* 39:1497-1504.

658 Sun C, Mchedlishvili Z, Bertram EH, Erisir A, Kapur J (2007) Selective loss of dentate hilar
659 interneurons contributes to reduced synaptic inhibition of granule cells in an electrical stimulation-
660 based animal model of temporal lobe epilepsy. *J Comp Neurol* 500:876-893.

661Sun C, Sun J, Erisir A, Kapur J (2014) Loss of cholecystokinin-containing terminals in temporal lobe
662 epilepsy. *Neurobiol Dis* 62:44-55.

663Thind KK, Yamawaki R, Phanwar I, Zhang G, Wen X, Buckmaster PS (2010) Initial loss but later
664 excess of GABAergic synapses with dentate granule cells in a rat model of temporal lobe epilepsy. *J*
665 *Comp Neurol* 518:647-667.

666Thom M, Zhou J, Martinian L, Sisodiya S (2005) Quantitative post-mortem study of the hippocampus in
667 chronic epilepsy: seizures do not inevitably cause neuronal loss. *Brain* 128:1344-1357.

668Tóth K, Eröss L, Vajda J, Halász P, Freund T, Maglóczy Z (2010) Loss and reorganization of
669 calretinin-containing interneurons in the epileptic human hippocampus. *Brain* 133:2763-2777.

670Upadhya D, Hattiangady B, Castro OW, Shuai B, Kodali M, Attaluri S, Bates A, Dong Y, Zhang S,
671 Prockop DJ, Shetty AK (2019) Human induced pluripotent stem cell-derived MGE cell grafting after
672 status epilepticus attenuates chronic epilepsy and comorbidities via synaptic integration. *PNAS*
673 116:287-296.

674Wennberg R, Arruda F, Quesney LF, Olivier A (2002) Preeminence of extrahippocampal structures in
675 the generation of mesial temporal seizures: evidence from human depth electrode recordings.
676 *Epilepsia* 43:716-726.

677West MJ, Slomianka L, Gundersen HJ (1991) Unbiased stereological estimation of the total number of
678 neurons in the subdivisions of the rat hippocampus using the optical fractionator. *Anat Rec* 231:482-
679 497.

680Williamson A, Patrylo PR, Spencer DD (1999) Decrease in inhibition in dentate granule cells from
681 patients with temporal lobe epilepsy. *Ann Neurol* 45:92-99.

682Wittner L, Maglóczy Z (2017) Synaptic reorganization of the perisomatic inhibitory network in
683 hippocampi of temporal lobe epileptic patients. *BioMed Res Intl* 2017:7154295.

684Wittner L, Maglóczy Z, Borhegyi Z, Halász P, Tóth S, Eröss L, Szabó Z, Freund TF (2001)
685 Preservation of perisomatic inhibitory input of granule cells in the epileptic human dentate gyrus.
686 *Neuroscience* 108:587-600.

687Zhang W, Buckmaster PS (2009) Dysfunction of the dentate basket cell circuit in a rat model of
688 temporal lobe epilepsy. *J Neurosci* 29:7846-7856.

689Zhang W, Yamawaki R, Wen X, Uhl J, Diaz J, Prince DA, Buckmaster PS (2009) Surviving hilar
690 somatostatin interneurons enlarge, sprout axons, and form new synapses with granule cells in a
691 mouse model of temporal lobe epilepsy. *J Neurosci* 29:14247-14256.

692Zhu Q, Mishra A, Park JS, Liu D, Le DT, Gonzalez SZ, Anderson-Crannage M, Park JM, Park G,
693 Tarbay L, Daneshvar K, Brandenburg M, Signoretti C, Zinski A, Gardner E, Zheng KL, Abani CP, Hu
694 C, Beaudreault CP, Zhang X, Stanton PK, Cho J, Velíšek L, Velíšková J, Javed S, Leonard CS, Kim
695 H, Chung S (2023) Human cortical interneurons optimized for grafting specifically integrate, abort
696 seizures, and display prolonged efficacy without over-inhibition. *Neuron* 111:807-823.

697Zhu ZQ, Armstrong DL, Hamilton WJ, Grossman RG (1997) Disproportionate loss of CA4 parvalbumin-
698 immunoreactive interneurons in patients with Ammon's horn sclerosis. *J Neuropathol Exp Neurol*
699 56:988-998.

700

701

702 Figure Legends

703 Figure 1 Adult female control sea lion hippocampus. Nissl stain (**A**), glutamic acid decarboxylase
704 (GAD)67-immunoreactivity to label cell bodies (**B**), and vesicular γ -amino butyric acid vesicular
705 transporter (VGAT)- plus GAD65/67-immunoreactivity to label synaptic boutons (**C**).

706
707 Figure 2 Control rat hippocampus processed for vesicular γ -amino butyric acid transporter (VGAT)-
708 plus glutamic acid decarboxylase (GAD)65/67-immunoreactivity to label synaptic boutons at low (**A**)
709 and high magnification (**B**). DG=dentate gyrus, G=granule cell layer, I=inner molecular layer, M=middle
710 molecular layer, O=outer molecular layer.

711
712 Figure 3 Plots of dentate gyrus volume (**A**), number of granule cells (**B**), glutamic acid decarboxylase
713 (GAD) cells (**C**), and GABAergic boutons per dentate gyrus (**D**) for individual hippocampi of control,
714 unilaterally sclerotic, and bilaterally sclerotic sea lions. Filled circles represent values of individual
715 hippocampi. Lines connect hippocampi from the same sea lion. Xs indicate group averages. Averages
716 for controls and bilateral sclerotic sea lions include both left and right hippocampi. Averages for
717 unilaterally sclerotic sea lions are plotted separately for sclerotic and non-sclerotic hippocampi. ^aversus
718 control and unilateral non-sclerotic, $p < 0.001$, ANOVA with Holm-Sidak method. ^bversus control and
719 unilateral non-sclerotic, $p < 0.05$, Kruskal-Wallis ANOVA on ranks with Dunn's method.

720
721 Figure 4 Dentate gyrus of an adult female control (**A,B**) and an adult female bilaterally sclerotic sea
722 lion (**C,D**). Nissl staining (**A,D**) reveals substantial loss of neurons in the hilus (H) and granule cell layer
723 (G) of the sclerotic hippocampus (**D**). **B** Glutamic acid decarboxylase (GAD)67-immunoreactivity shows
724 many GAD cells in the hilus of the control sea lion and some in the granule cell layer and molecular
725 layer (M). **C** There are fewer GAD cells in the sclerotic hippocampus, especially in the hilus.

726
727 Figure 5 Distribution of glutamic acid decarboxylase (GAD)-immunoreactive cell profiles in layers of the
728 dentate gyrus and along the septotemporal axis of the hippocampus. Number (**A**) and proportion (**B**) of

729 GAD cell profiles in layers of the dentate gyrus. Bars represent averages of non-sclerotic (control and
730 unilateral non-sclerotic) and sclerotic (bilateral and unilateral sclerotic) hippocampi. Markers indicate
731 individuals. Error bars indicate 95% confidence interval. ^ap<0.0001, t test; ^bp=0.002, ^cp=0.045, Mann-
732 Whitney rank sum test. **C** Number of GAD cell profiles per section along the septotemporal axis in non-
733 sclerotic and sclerotic hippocampi. Values represent mean ± 95% confidence interval. 0%
734 septotemporal distance = septal pole; 100% = temporal pole.

735
736 Figure 6 Dentate gyrus of the non-sclerotic (**A-C**) and sclerotic (**D-F**) hippocampi of a subadult female
737 sea lion. Nissl staining (**A,D**) reveals neuron loss in the hilus (H) and granule cell layer (G) of the
738 sclerotic hippocampus. Immunolabeling for γ-amino butyric acid vesicular transporter (VGAT) plus
739 GAD65/67 (**B,C,E,F**) reveals GABAergic synaptic boutons. M=molecular layer, I=inner molecular layer.
740

741 Figure 7 Distribution of γ-amino butyric acid vesicular transporter (VGAT)- plus glutamic acid
742 decarboxylase (GAD)65/67-immunoreactive synaptic boutons in layers of the dentate gyrus and along
743 the septotemporal axis of the hippocampus. Number (**A**) and proportion (**B**) of GABAergic boutons in
744 layers of the dentate gyrus. Bars represent averages of non-sclerotic (control and unilateral non-
745 sclerotic) and sclerotic (bilateral and unilateral sclerotic) hippocampi. Markers indicate individuals. Error
746 bars indicate 95% confidence interval. *p<0.001, Mann-Whitney rank sum test. **C** Number of
747 GABAergic boutons per section along the septotemporal axis in non-sclerotic and sclerotic hippocampi.
748 Values represent mean ± 95% confidence interval. 0% septotemporal distance = septal pole; 100% =
749 temporal pole.

750
751 Figure 8 Scatter plots with regression lines of correlated pathological parameters (see text for
752 statistical analysis). Markers indicate values of individual hippocampi. **A** Dentate gyrus volume versus
753 number of granule cells. **B** Dentate gyrus volume versus number of GABAergic boutons. **C** Number of
754 granule cells versus number of GABAergic boutons. The regression line y-intercept is 1.14×10^9
755 boutons, and the slope is 2030 boutons per granule cell.

eNeuro Accepted Manuscript

757 Table 1 Parameters of optical fractionator analyses.

758

	Counting frame (µm)	Counting grid (µm)	Dissector height	Average sections analyzed	Average caps counted	Coefficient of variation	Mean coefficient of error*
Granule cells**	10x10	150x150	Total section thickness	10	152	0.72	0.14
GAD cells	100x100	500x500 or 350x350***	Total section thickness	10	198	0.54	0.07
GABAergic boutons - Sea lions	5x5	800x800	1 µm	10	1079	0.59	0.07
GABAergic boutons - rats	5x5	400x400	1 µm	10	921	0.10	0.05

759

760 *Calculated according to West et al. (1991).

761 **From Cameron et al. (2019).

762 ***Shrunken hippocampi were analyzed with a counting grid of 350x350 µm so enough GAD
763 cells could be sampled.

764

765

766 Table 2 Dentate gyrus volume and numbers of granule cells, glutamic acid decarboxylase (GAD)-
 767 positive interneurons, and γ -amino butyric acid (GABA)ergic boutons per dentate gyrus in control sea
 768 lions and sea lions with unilateral or bilateral hippocampal sclerosis. Values represent mean \pm 95%
 769 confidence interval.

770

771

	Control	Unilateral non-sclerotic	Unilateral sclerotic	Bilateral sclerotic
Animals/hippocampi	13/26	8/8	8/8	8/16
Dentate gyrus volume	91.8 \pm 6.6	106.1 \pm 17.8	47.9 ^a \pm 14.6	54.3 ^a \pm 7.9
Granule cells	2,318,000 \pm 181,000	2,382,000 \pm 409,000	627,000 ^a \pm 494,000	459,000 ^a \pm 309,000
GAD neurons	244,400 \pm 23,000	230,100 \pm 46,900	45,700 ^a \pm 13,100	87,400 ^a \pm 22,600
GABAergic boutons ($\times 10^9$) [*]	5.67 \pm 0.83	6.90 \pm 2.61	2.58 ^b \pm 1.34	1.84 ^b \pm 0.38

772

773^{*}Includes granule cell layer and molecular layer, not hilus.

774^aversus control and unilateral non-sclerotic, $p < 0.001$, ANOVA with Holm-Sidak method.

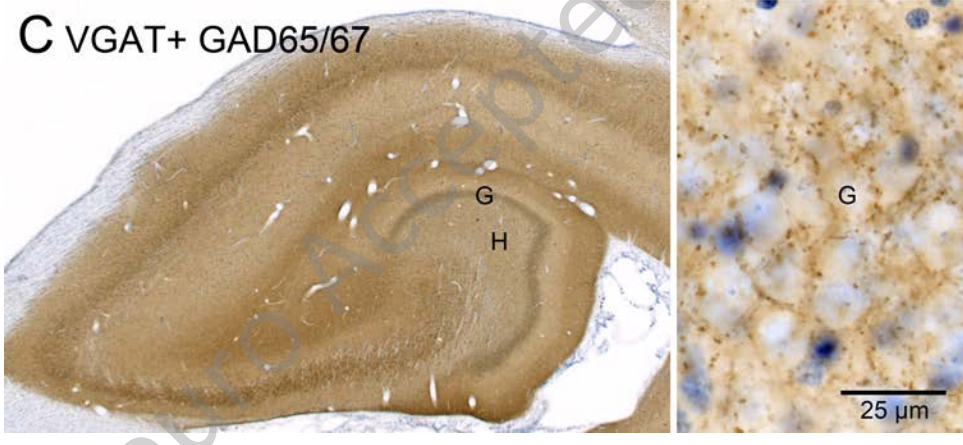
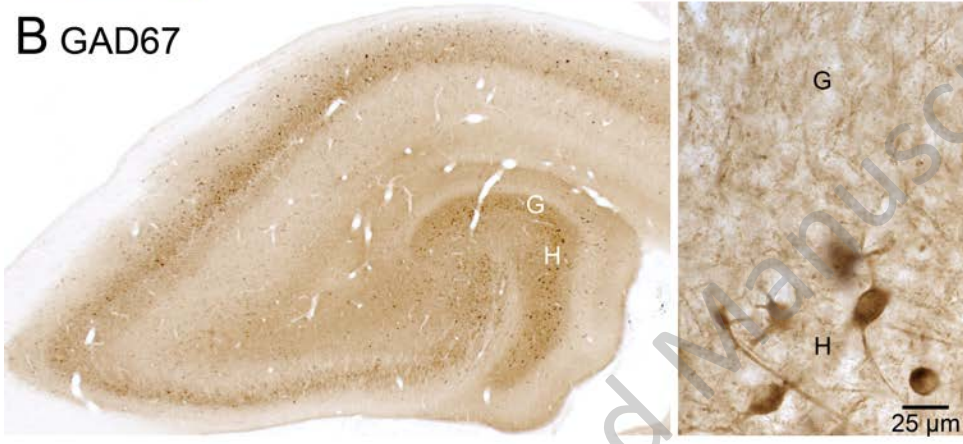
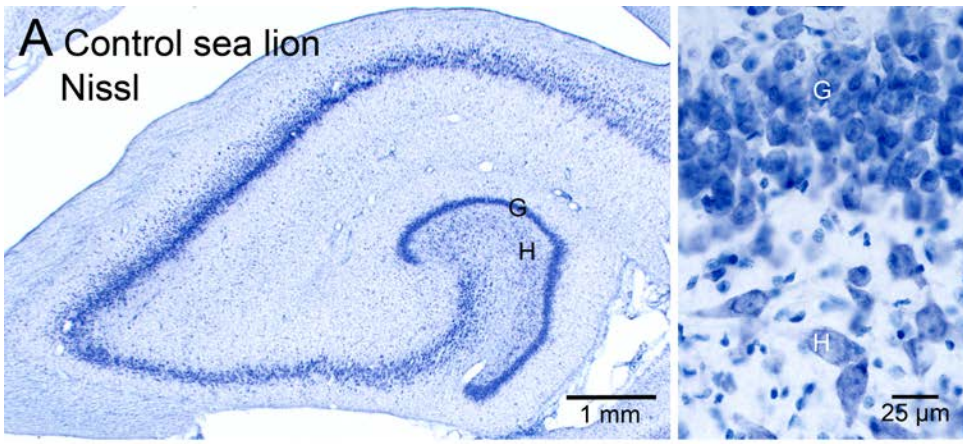
775^bversus control and unilateral non-sclerotic, $p < 0.05$, Kruskal-Wallis ANOVA on ranks with Dunn's

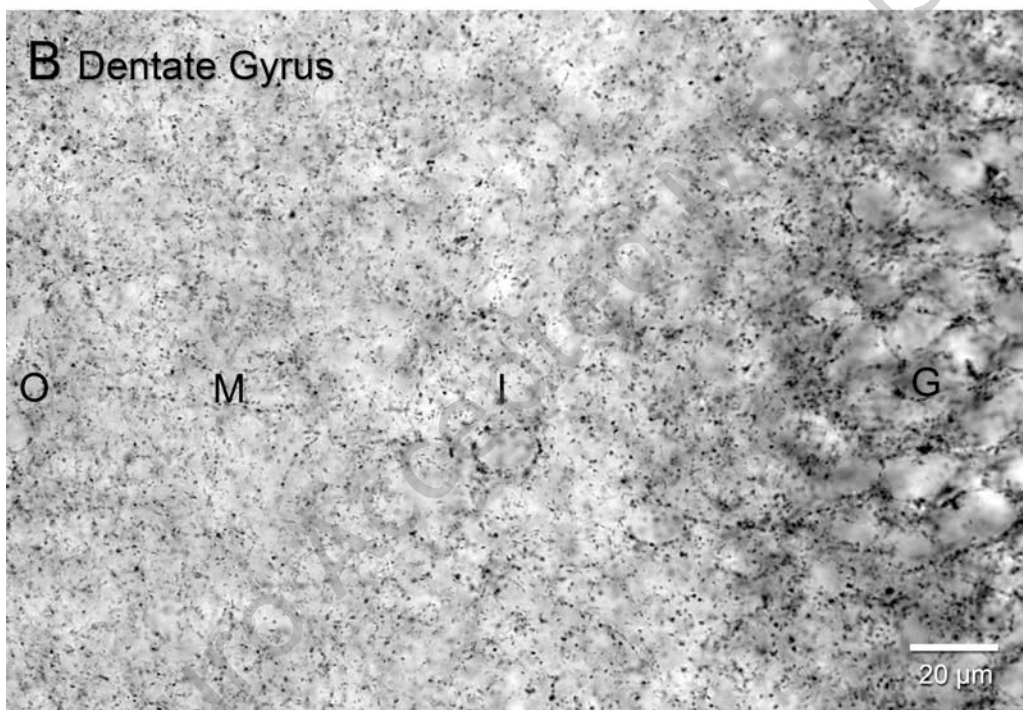
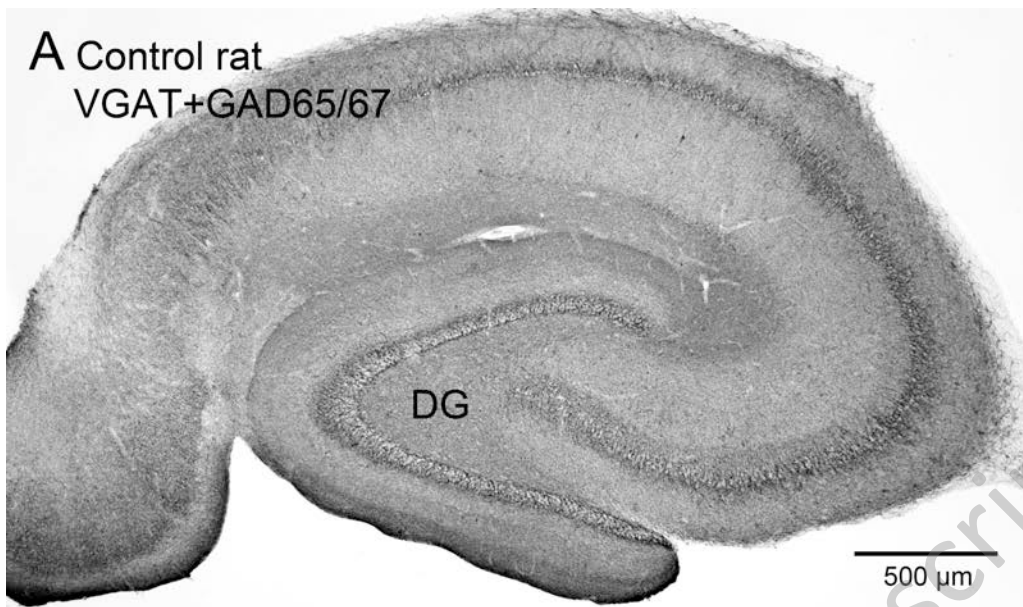
776 method.

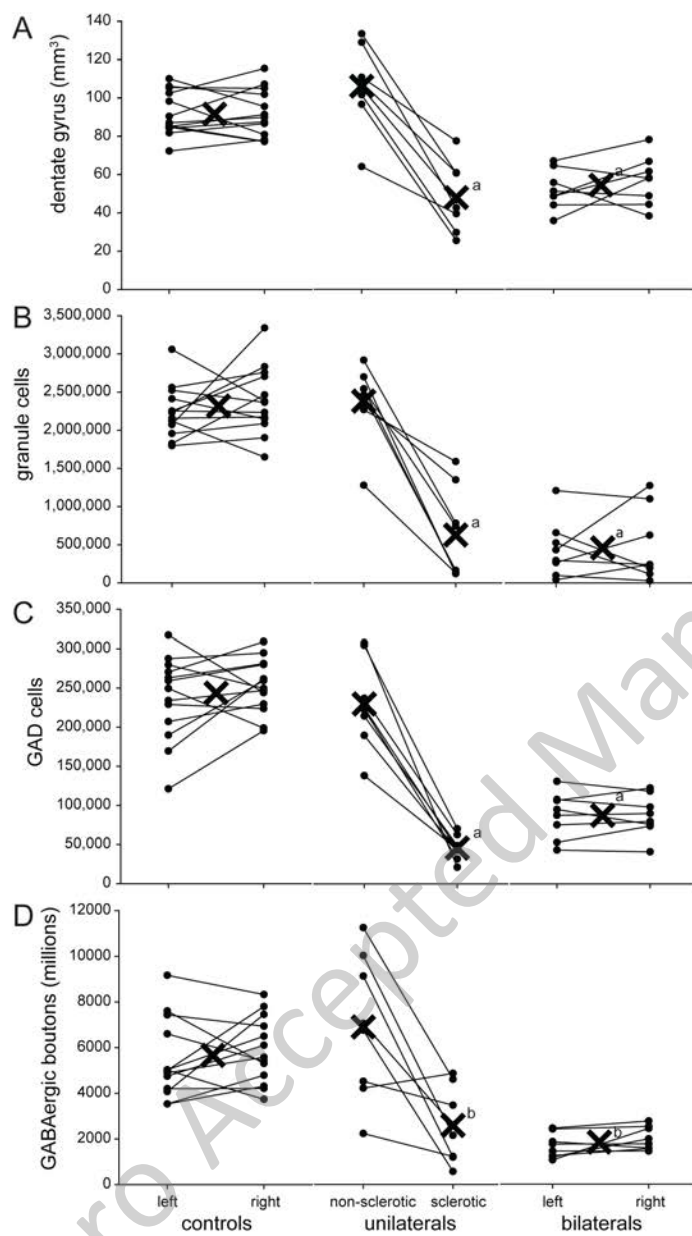
777

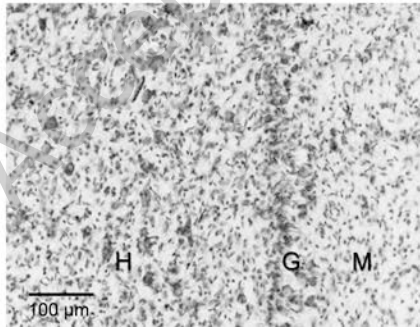
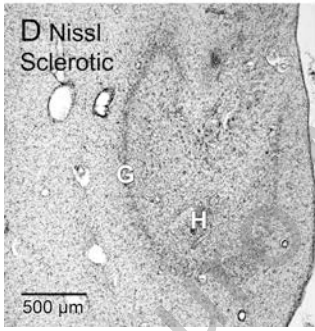
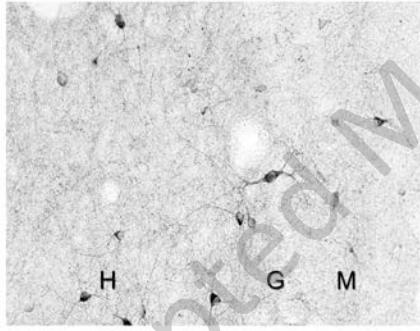
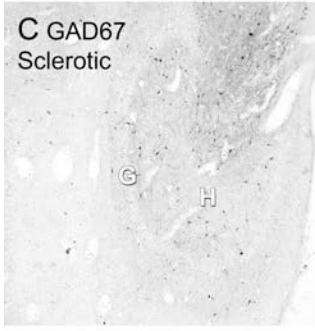
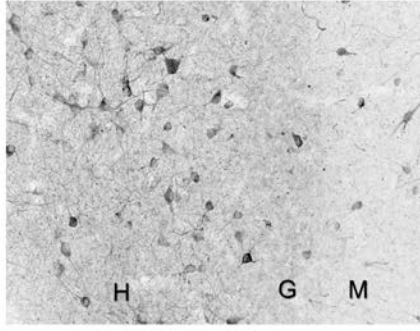
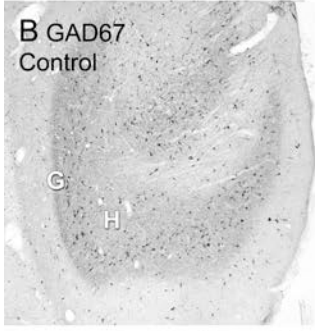
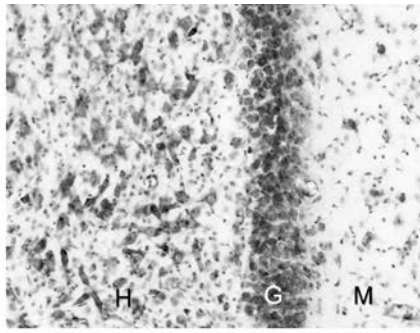
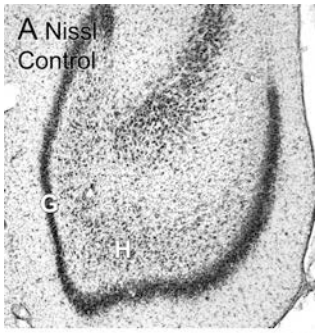
778

779









eNeurology Accepted Manuscript

